Crystallization process and magnetic properties of $Fe_{100-x}B_x$ ($10 \leqq x \leqq 35$) amorphous alloys and supersaturated state of boron in α-Fe

TOSHIO NAKAJIMA
R & D Laboratory, TOPY Industries Ltd, 1 Akemi-cho, Toyohashi, Aich Prefecture 440, Japan
EIJI KITA
Institute of Applied Physics, University of Tsukuba, Sakura-mura, Ibaraki Prefecture 305, Japan
HIROMITSU INO
Department of Materials Science, Faculty of Engineering, University of Tokyo, 7-3-1, Hongo, Bunkyo-ku, Tokyo 113, Japan

Amorphous specimens of $Fe_{100-x}B_x$ were prepared in the range $10 \leqq x \leqq 35$ at% B by a single-roller method. The crystallization process and the boron concentration dependence of the Curie temperature were examined by differential scanning calorimetry, X-ray diffraction, Mössbauer spectroscopy and magnetic measurements. Two-step crystallization was observed in specimens with $x < 17$: amorphous → amorphous + boron-supersaturated bcc phase (α-Fe(B)) → t-Fe_3B + α-Fe. A single α-Fe(B) phase was not observed. The transition temperature from t-Fe_3B to stable (α-Fe + t-Fe_2B) sensitively depends on the boron content in the alloys. The crystallization temperature (T_x) of the amorphous alloys was almost unchanged for $17 \leqq x \leqq 31$, but increased remarkably at high boron concentrations of $x \geqq 33$, where the decomposition products consisted of t-Fe_2B and o-FeB. The Curie temperature (T_c) of the amorphous phase was as low as 480 K at $x = 10$, increased with increasing boron content up to 820 K and then decreased in the high boron concentration alloys of $x > 28$. A single α-Fe(B) phase was not detected in the as-quenched specimens of $x = 8$ and 10. The phase coexisted with the o-Fe_3B and amorphous phases. The lattice parameter of the phase was 0.2861_0 nm which was smaller than that of pure iron by 2/1000, indicating the substitutional occupation of boron atoms in the bcc lattice.

1. Introduction

It has been recognized that a study of the Fe–B alloy system is important as a basis of industrial application of iron-based ternary amorphous alloys. Much work has been carried out [1–6], but several problems remain to be clarified. The crystallization of $Fe_{100-x}B_x$ amorphous alloys containing less than 17 at% B occurs by two stages of reaction, and different results have been reported for the formation of the intermediate phases. It is also interesting to know the behaviour of the Curie temperature T_c at high boron concentrations of $x > 26$, since it has been shown that T_c increases with increasing boron in the range $12 \leqq x \leqq 26$ at% B [7].

The equilibrium solid solubility of boron in α-Fe is extremely small, i.e. less than 0.04 at%. Therefore, it is difficult by the usual methods to investigate whether the solute atoms occupy substitutional or interstitial sites. The ratio of the atomic radius of boron and α-Fe (R_B/R_{Fe}) is 0.73. This value is smaller than the limit of the favourable value (0.85 to 1.15) for the formation of a substitutional alloy (Hume-Rothery's value), and is larger than 0.59, the maximum value for interstitial alloy compounds (Hägg's rule).

If a solid solution with high boron supersaturation (α-Fe(B)) can be obtained by liquid quenching, it will be clarified which type of solution takes place. In this respect Ray and Hasegawa [8] measured the lattice parameters and densities of liquid-quenched Fe–B alloys and concluded that the boron atoms occupy both substitutional and interstitial sites of the bcc lattice. However, their interpretation seems to be not conclusive, because a measured value of density only gives the average for the specimen, which is strongly disturbed by the coexistence of a small amount of secondary phase such as amorphous material or a compound.

In this work, the crystallization process and Curie temperature are studied for $Fe_{100-x}B_x$ ($10 \leqq x \leqq 35$) amorphous alloys, the composition range of which is wider than in previous work. The bcc solid solution with boron supersaturation is also investigated.

2. Experimental procedures

Mother alloys with 4 to 40 at% B were fabricated in the shape of buttons by arc-melting electrolytic iron (99.9 wt% purity) and crystalline boron (99.5 wt% purity) in an argon atmosphere. Each alloy was ca.

0022-2461/88 $03.00 + .12

40 g in weight. Specimens with a weight of 1 to 3 g for one charge were prepared by a single-roller method. A copper roller with a diameter of 250 mm was used and the speed of the roller surface was varied between 39 and 91 m sec^{-1}. The ejection gas pressure, the difference in pressure between the spinning chamber and the gas tank, was controlled between 20 and 40 kPa. The gap between the crucible bottom and the roller surface was adjusted to 0.2 to 0.3 mm.

A quartz crucible of 10 mm diameter with an orifice was used. A suitable dimension for the orifice was selected depending on the boron content of the sample. A slit orifice with a size of 0.35 mm × 3.0 mm was used for $12 \leqq x \leqq 28$ at % B in which the amorphous state is considered relatively easy to obtain. The section of the ribbon specimens was ca. 2.7 mm in width and ca. 15 μm in thickness. For $x < 12$ and $x > 28$, liquid quenching was carried out by using an orifice with a diameter of 0.4 mm. The ribbons were 0.3 to 0.4 mm wide and ca. 10 μm thick.

The boron concentration of specimens was determined by a sodium hydroxide titration method (JIS G 1327: analytical method for ferroboron alloy). The crystallization temperature (T_x) of the amorphous alloys was examined by a differential scanning calorimeter (DSC) at a heating rate of 0.33 K sec^{-1} in an atmosphere of pure argon gas enclosing the specimen (7 to 10 mg) in a silver pan. X-ray diffraction and Mössbauer effect measurements were also done on both as-quenched and heat-treated specimens.

X-ray diffraction peak angles of the as-quenched Fe–B supersaturated solid solution were measured by a step scanning method (2θ interval 0.17 mrad (0.01°), counting time 40 sec per step, intensity of X-rays 40 kV × 20 mA), and compared with those of pure iron.

The Curie temperature (T_c) was measured using a magnetic balance in a field of 0.1 T and in the temperature range between room temperature and 1103 K at a heating rate of 0.028 to 0.036 K sec^{-1}. A specimen with 0.8 to 1.6 mg weight was heated in a helium atmosphere of several hundred pascals.

3. Results and discussion

3.1. Phase analysis of as-quenched alloys

In the liquid quenching of $Fe_{100-x}B_x$ alloy, the formation of amorphous material in the range $x = 12$ to 28 has been reported in previous papers [3, 7]. In these experiments, the amorphous state was difficult to obtain at low boron contents of $x < 12$, as also mentioned in the literature. On the other hand, amorphous specimens have been fabricated in this laboratory up to 35 at % on the high boron side, as we reported in a short note [9]. The most important factor for increasing the cooling rate seems to be a good contact between melt and roller surface, attained by the lack of gas bubbles when the specimen is quenched in a vacuum. Amorphous alloys containing high boron contents of $x > 28$ were made in a slim ribbon shape (0.3 to 0.4 mm wide and 7 to 10 μm thick) when the speed of roller surface was 65 m sec^{-1} and the ejection gas pressure was 30 kPa (ca. 0.3 atm).

Fig. 1 shows X-ray diffraction patterns of as-quenched specimens ($x = 4$ to 12). The specimens of $x = 4$ and 6 consisted of α-Fe and o-Fe_3B. The formation of supersaturated solid solution was confirmed in the as-quenched specimen of $x = 8$ from the decrease in lattice parameter. The coexistence of the α-Fe(B) and o-Fe_3B phases in the specimen of $x = 8$ was shown by increasing the sensitivity of X-ray detection (Fig. 2).

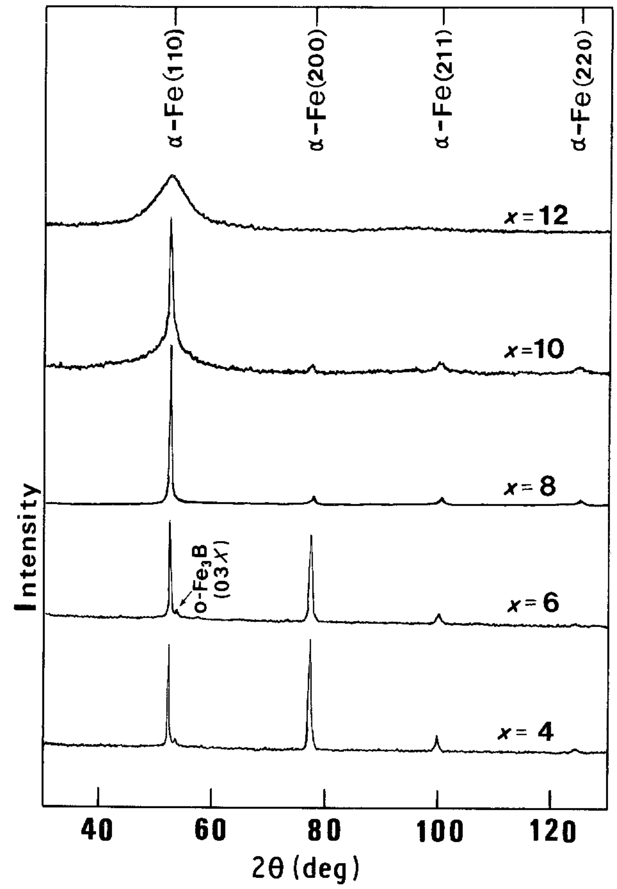

Figure 1 X-ray diffraction patterns (CoKα radiation) of as-quenched specimens for $Fe_{100-x}B_x$ (x = 4, 6, 8, 10 and 12).

For the as-quenched specimen of $x = 10$, it was

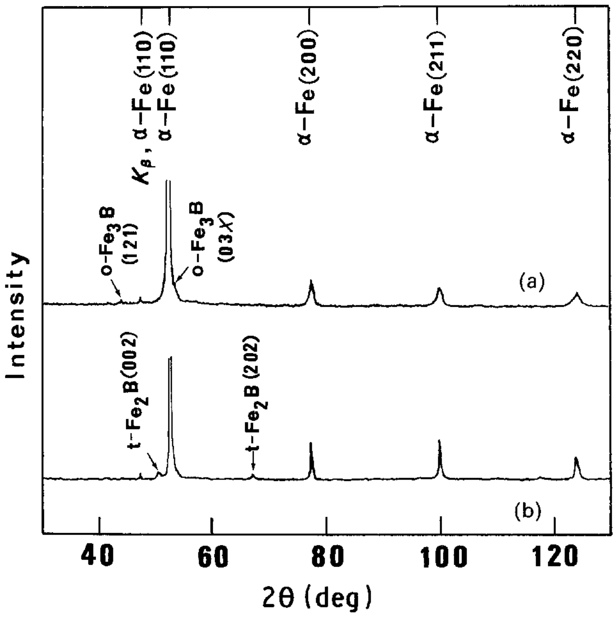

Figure 2 X-ray diffraction patterns (CoKα radation) of $Fe_{92}B_8$ (a) as-quenched and (b) aged at 873 K for 600 sec.

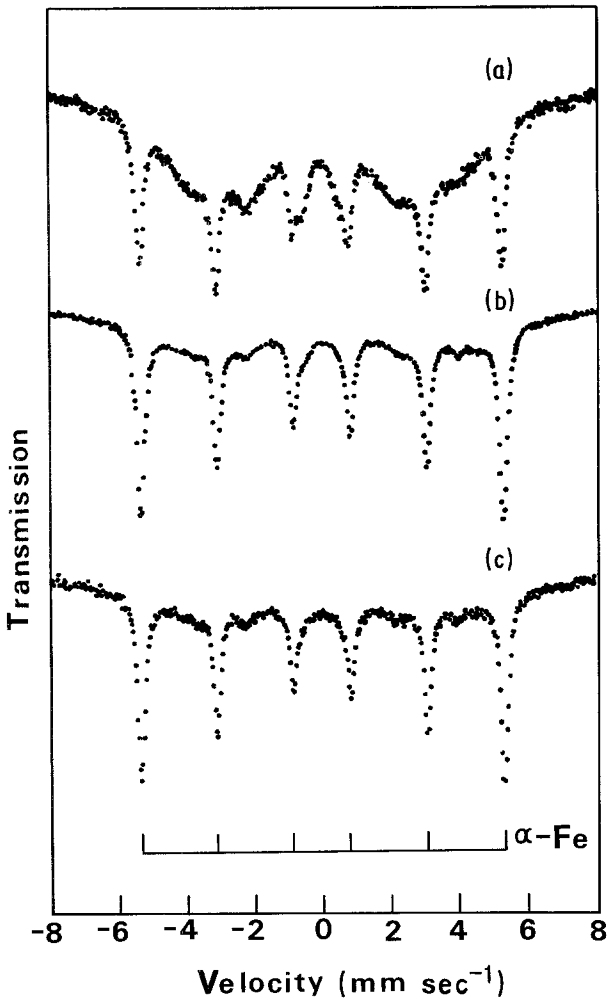

Figure 3 Mössbauer spectra of as-quenched $Fe_{100-x}B_x$ at 300 K: (a) $Fe_{90}B_{10}$, (b) $Fe_{92}B_8$, (c) $Fe_{94}B_6$.

confirmed from the following experimental results that the amorphous phase was contained together with α-Fe(B): (i) the skirt of the X-ray diffraction peak of α-Fe was broad, (ii) the Mössbauer spectrum consisted of a sextet of α-iron and a broad component (Fig. 3), and (iii) exothermic peaks due to crystallization were detected in the DSC profile (see Fig. 5 below). In addition, a lattice parameter change of the bcc phase was observed as well as at $x = 8$. From those results, the as-quenched specimen of $x = 10$ seems to consist of supersaturated α-Fe(B) and amorphous phases. Nevertheless, the coexistence of a third phase with a high boron concentration would be predicted from the balance of total boron content, because of the following two facts: (i) the boron concentration of α-Fe(B) is estimated to be less than 1 at % from the change in lattice parameter, and (ii) the boron content of the amorphous phase is presumed to be little changed from the original value of ca. 10 at % from the measurement of T_x and T_c, as concluded below in Sections 3.2 and 3.4, respectively. The excess boron atoms excluded from α-Fe(B) would be contained in fine particles of a third phase such as o-Fe_3B, although this phase was not detected by X-ray diffraction.

Single amorphous alloys were obtained in the range of 12 to 35 at % B. The specimens of 12 to 28 at % B were fabricated in the shape of continuous ribbons with good toughness. However, ribbons with high boron ($x = 31$, 33 and 35) were brittle and not continuous (10 to 50 mm in length). For $x = 38$ and 40, the amorphous state could not be attained. The as-quenched state was a mixture of t-Fe_2B and o-FeB.

3.2. Supersaturated state of boron in α-Fe

Step scanning measurements showed that the diffraction peaks of α-Fe shifted to the high angle side in specimens of $x = 8$ and 10. For $x = 8$, the peak angles of the (1 1 0), (2 0 0), (2 1 1) and (2 2 0) reflections of α-Fe shifted by +3.1 mrad (0.18°), +4.7 mrad (0.27°), +5.2 mrad (0.30°) and +7.7 mrad (0.44°), respectively.

The lattice parameter of the bcc lattice for the as-quenched specimen of $x = 8$ was determined by an extrapolation method, together with that of the heat-treated specimen, as shown in Fig. 4. In the

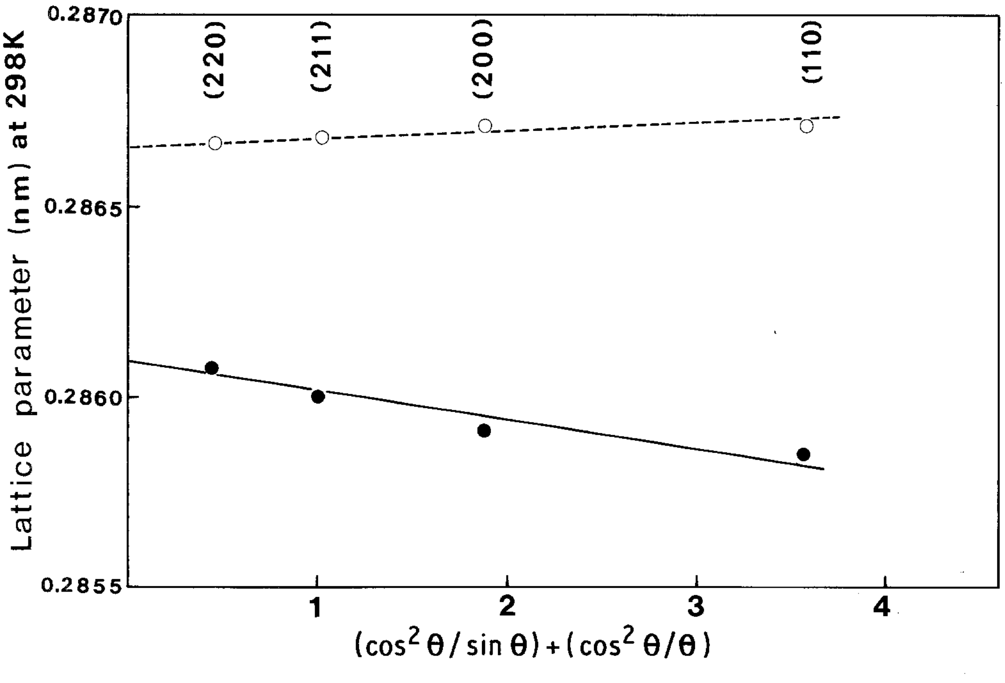

Figure 4 Derivation of lattice parameters of $Fe_{92}B_8$ (●) as-quenched and (○) aged at 873 K for 600 sec.

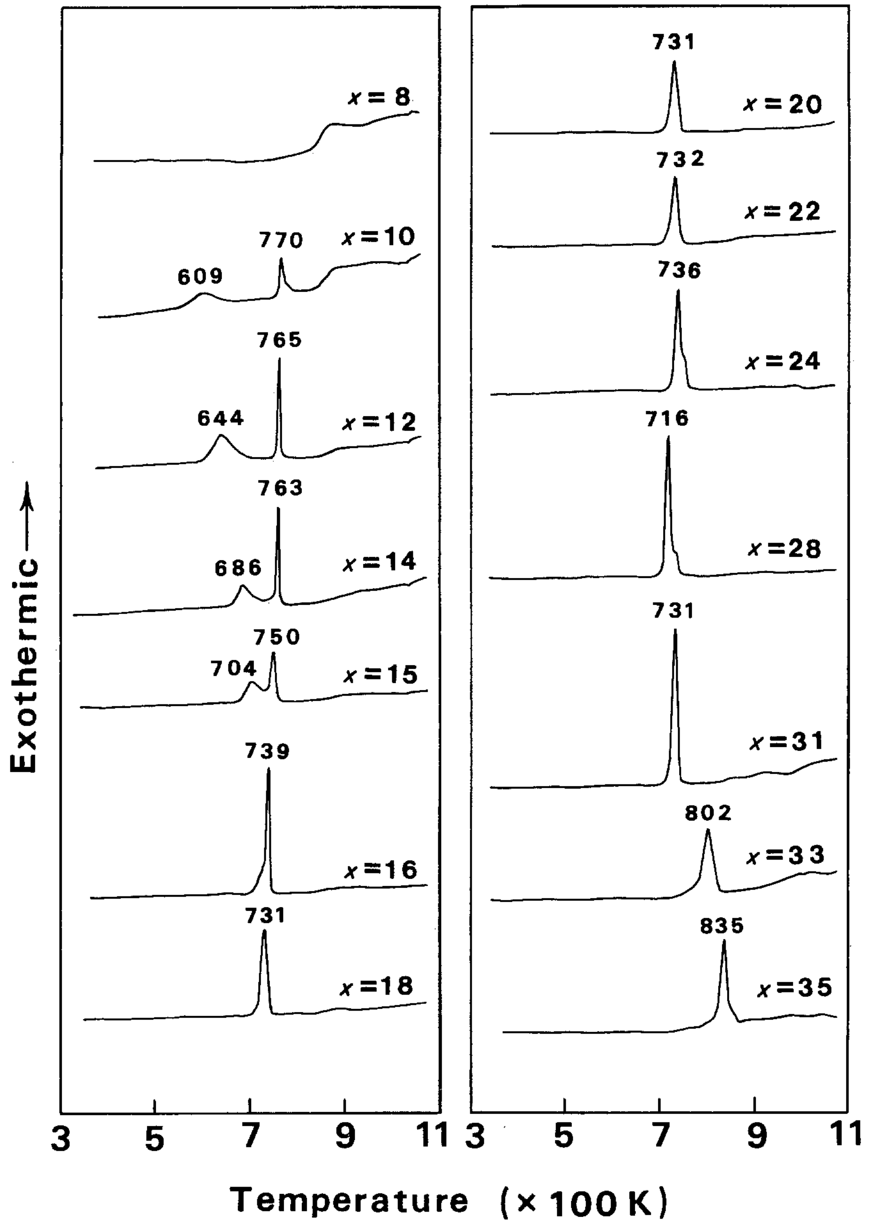

Figure 5 Thermograms of as-quenched $Fe_{100-x}B_x$ alloys (x = 8 to 35 at % B, heating rate 0.33 K sec^{-1}).

as-quenched state, the value was determined as 0.2861_0 nm (at 298 K), which is smaller than for pure iron (0.2866_3 nm at 298 K) by ca. 0.2%. After heating up to 873 K, the value was nearly the same as for pure iron, where the phases were changed to stable α-Fe and t-Fe_2B (see Fig. 2). For the as-quenched specimen of $x = 10$, the lattice parameter was determined to be 0.2861_0 nm (at 298 K). In the specimens of $x = 4$ and 6, the values were 0.2866_7 and 0.2866_8 nm (at 298 K), respectively, which were in good agreement with that of pure iron within the error range.

Ray and Hasegawa [8] have previously studied liquid-quenched specimens of 4 to 12 at % B. The lattice parameter for 8 at % B reported by them is in good agreement with the present value of 0.2861 nm. In their paper, however, the as-quenched state was interpreted to be a single α-Fe(B) phase, and all the boron atoms were assumed to occupy substitutional and interstitial sites of the α-Fe lattice. On the contrary, in our experiments the formation of a two-phase mixture of α-Fe(B) and o-Fe_3B was clearly observed at $x = 8$ as previously described. The boron atoms dissolved in α-Fe(B) were estimated to be ca. 1 at %, assuming that the lattice parameter of the substitutional solid solution changed according to Vegard's law.

3.3. *The crystallization process*

3.3.1. *Crystallization temperature* (T_x)

Fig. 5 shows thermograms of liquid-quenched specimens at a heating rate of 0.33 K sec^{-1}. The concentration of T_x in the range of 12 to 24 at % B showed the tendency as previously reported [10] and T_x is nearly constant up to 31 at %. However, the crystallization temperature increased remarkably at a boron content of 33 at %, and T_x for $x = 35$ was as high as 835 K (562° C). This value is higher than the crystallization temperature of $x = 18$ to 31 by ca. 100 K. It would be probable that the increase in T_x is related to the absence of α-Fe phase in the crystallized phase, and much time is necessary for the formation of any compound phase with a complicated structure in comparison with that of α-Fe.

Amorphous $Fe_{100-x}B_x$ alloys have previously been fabricated by r.f. sputtering in the wider and higher composition range from 10 to 90 at % B [11]. It has also been reported that the crystallization temperatures of the sputtered films increased gradually with

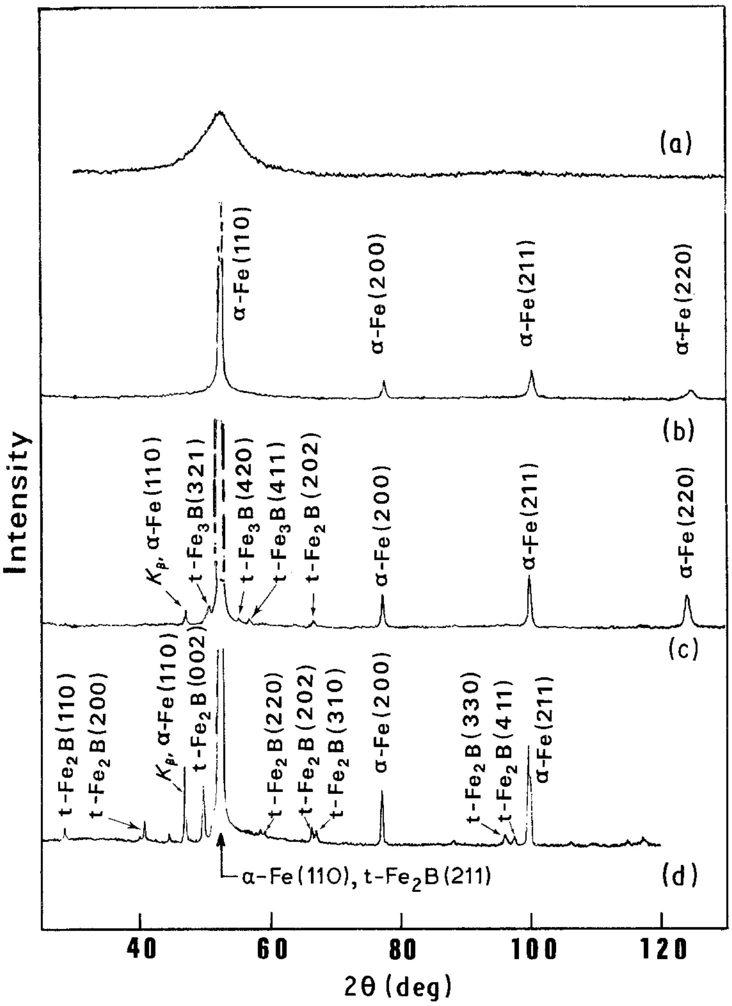

Figure 6 X-ray diffraction patterns (Co$K\alpha$ radiation) of $Fe_{88}B_{12}$ (a) as-quenched, and aged in three temperature ranges: (b) up to 673 K, (c) up to 783 K, (d) up to 903 K.

increasing boron content up to 36 at % B and then rapidly decreased [12]. The present experiments on liquid-quenched $Fe_{100-x}B_x$ amorphous alloys showed that the crystallization temperatures (for a heating rate of 0.33 K sec^{-1}) were approximately 50 to 70 K higher at $x = 33$ and 35 than those for sputtered samples (for 0.17 K sec^{-1}) of the same compositions. The difference in T_x influenced by the heating rate (0.17 and 0.33 K sec^{-1}) was estimated to be about 14 K from the DSC measurements. Therefore the crystallization temperatures of amorphous alloys prepared by liquid quenching were higher by ca. 35 to 55 K in this composition range. Although the reason for the discrepancy is not clear, it is supposed that gas contamination or internal stress in the sputtered films acts to lower the crystallization temperature.

3.3.2. Crystallization sequence

3.3.2.1. Specimens of $x < 17$. The intermediate state between the first and second crystallization steps was studied in detail especially for a specimen of $x = 12$, because of the wide temperature interval between the two exothermic peaks (T_{x1} and T_{x2}) in the DSC profile.

Fig. 6 shows X-ray diffraction patterns for annealed specimens of $x = 12$, together with that of the as-quenched one. As can be seen in this figure, the only phase detected was the b c c phase after heating up to 673 K (at a heating rate of 0.33 K sec^{-1}). Fig. 7 shows lattice parameters for the annealed specimens of $x = 12$, together with that of pure iron. In the specimen after heating up to 673 K, the extrapolated value was 0.2860$_0$ nm (at 292 K) which was smaller than that of pure iron. The lattice parameter after further heating up to 783 K, the second crystallization temperature, increased to the same value as pure iron (0.2866$_1$ nm at 292 K).

Takahashi *et al.* [3] have reported that a single phase of α-Fe(B) was obtained in a heat-treated specimen of 12 at % B (up to 663 K, at 0.028 K sec^{-1}) and that the lattice parameter was 0.2855 nm. The value approximately agrees with our result, but the phase analysis is different. From Mössbauer spectra measurements for heat-treated specimens of $x = 12$, the formation of the amorphous phase together with α-Fe(B) was certainly confirmed. Fig. 8 shows the result for a specimen annealed up to 673 K. After annealing up to a higher temperature by 30 K (703 K) at a heating rate of 0.33 K sec^{-1}, the amorphous component was also observed in the Mössbauer spectrum. X-ray diffraction of the same specimen indicated just the same lattice parameter of 0.2860$_0$ nm (at 292 K) of the b c c phase as that measured in the specimen annealed up to 673 K. In this study, we concluded that the state is the mixture of amorphous and α-Fe(B) phases in the temperature range between T_{x1} and T_{x2}.

3.3.2.2. $17 < x < 25$. It was shown that the temperature at which the metastable t-Fe_3B changes to the stable state sensitivity depends on the boron content. Fig. 9 shows the X-ray diffraction patterns of $x = 12$, 18 and 24 after heating up to 903 K. These specimens were annealed in a vacuum in the same

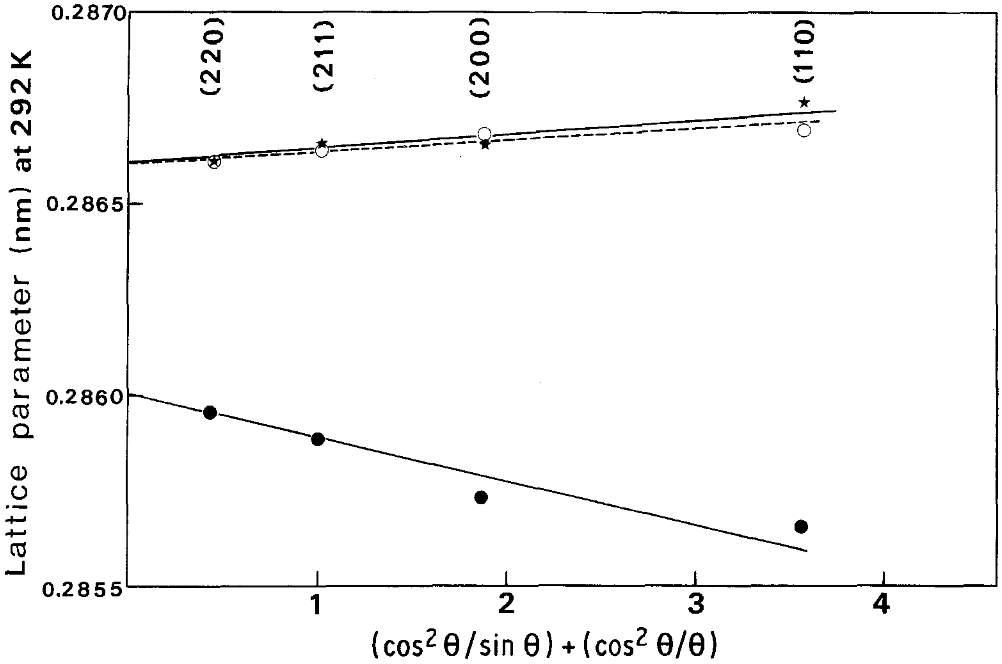

Figure 7 Derivation of lattice parameters of $Fe_{88}B_{12}$, aged up to (●) 673 K and (○) 783 K, and (★) pure α-iron as reference.

capsule made of nickel. The stable phases (α-Fe and t-Fe_2B) existed in the annealed specimens of $x = 12$ and 24. On the other hand, the metastable phase remained in the specimen of $x = 18$. Since the thermal change from metastable to stable was hardly detected in the profiles of DSC, each specimen was annealed up to various temperatures at the same heating rate of ca. 0.33 K sec^{-1} and analysed by X-ray diffraction. The phase analyses showed that the highest transition temperature was around $x = 20$. This result indicated the same tendency as shown by Takahasi *et al.* [3]. However, the o-Fe_3B phase reported in the literature was not detected in this work in the whole crystallization process from amorphous to final state. The reactions for the alloys of $17 < x < 25$ are concluded to be amorphous → α-Fe + t-Fe_3B → α-Fe + t-Fe_2B. The formation of a single Fe_3B phase by polymorphic reaction as suggested by Köster and Herold [13] was not confirmed in this experiment. No specimen with exactly stoichiometric concentration ($x = 25$) was prepared. However, it is noticed that the formation of t-Fe_2B phase is easy and stable compared with *t*-Fe_3B in the vicinity of $x = 25$ as shown in Fig. 10.

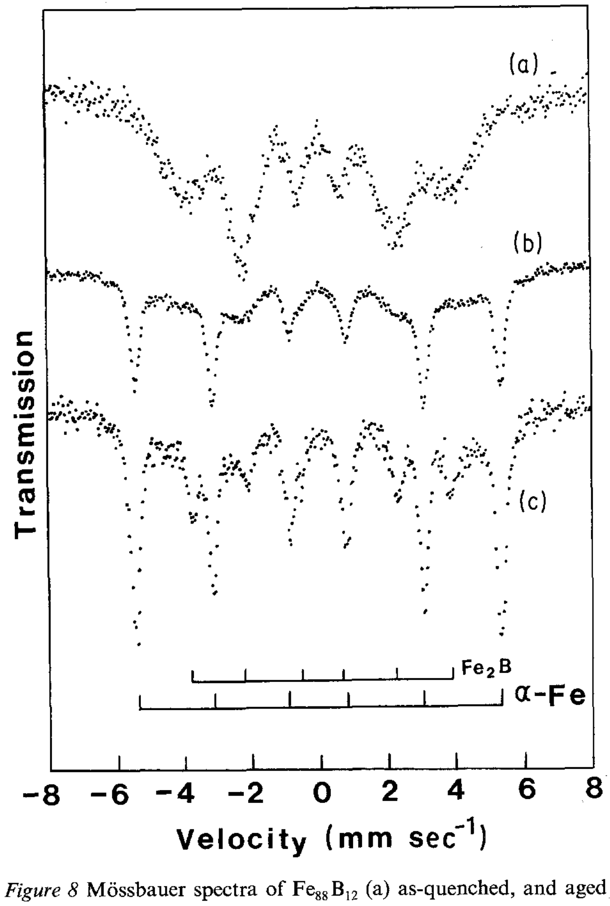

Figure 8 Mössbauer spectra of $Fe_{88}B_{12}$ (a) as-quenched, and aged up to (b) 673 K and (c) 783 K.

3.3.2.3. $x > 25$. X-ray diffraction and Mössbauer effect measurements for specimens aged at a temperature just above the exothermic DSC peak showed that the crystallization progresses by the following reactions [9]: amorphous → α-Fe + t-Fe_2B for $x = 28$, amorphous → t-Fe_2B for $x = 33$, and amorphous → t-Fe_2B + o-FeB for $x = 35$. A summarized phase diagram for the crystallization is shown in Fig. 10.

3.4. Magnetic measurements

Fig. 11 shows the magnetization against temperature curves which were measured by a magnetic balance at a heating rate of 0.028 to 0.036 K sec^{-1} for specimens of $x = 10$ to 35. Concentration dependences of T_x and T_c determined from the magnetic measurements are summarized in Fig. 12. The Curie temperature T_c of the amorphous alloy increased with increasing boron content in the range of $x < 26$, the tendency already shown in previous reports [3, 7]. It becomes clarified in this paper that the Curie temperature decreases in the high boron content of $x > 28$.

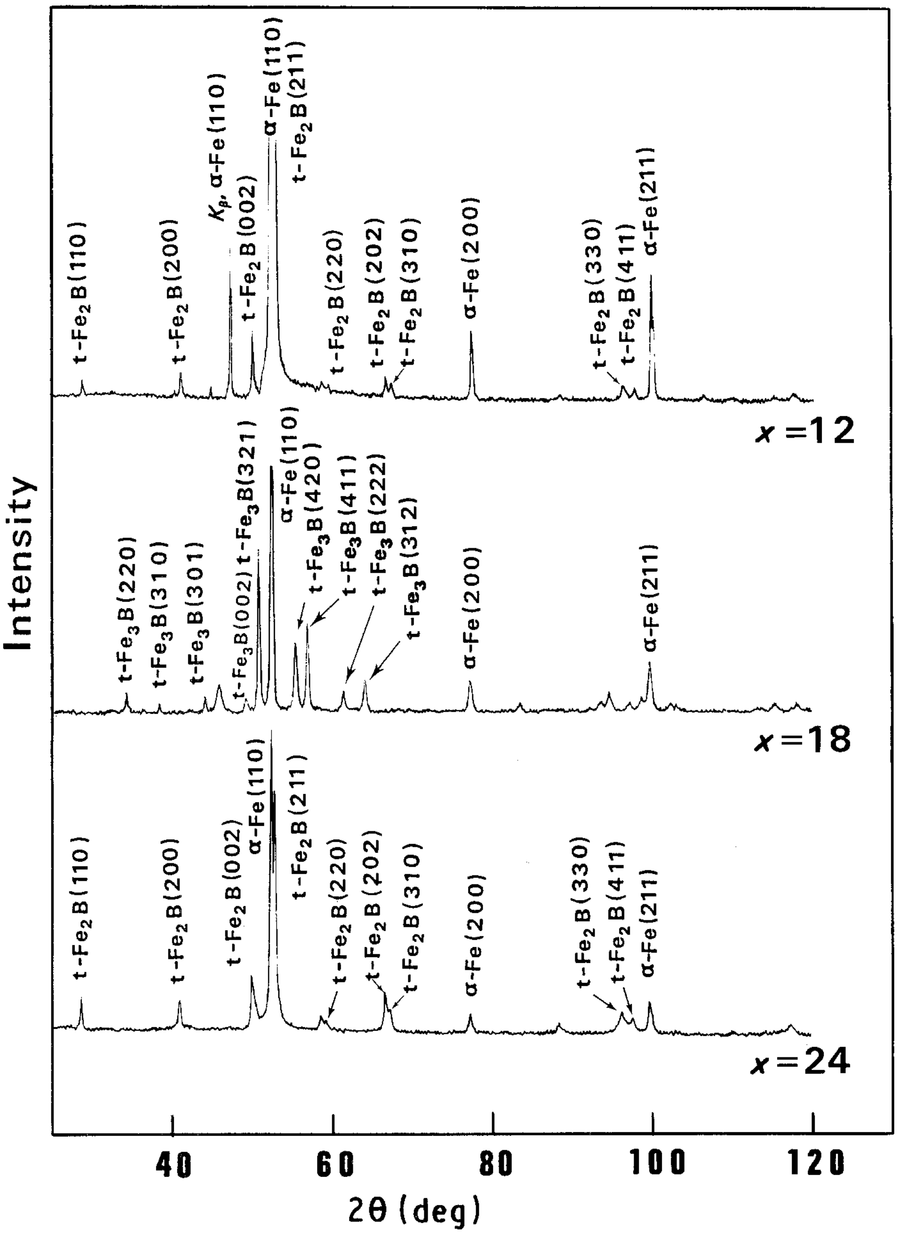

Figure 9 X-ray diffraction patterns (Co$K\alpha$ radiation) of crystallized $Fe_{100-x}B_x$ (x = 12, 18 and 24) alloys after heating up to 903 K.

3.4.1. Determination of Curie temperature of amorphous phase

The Curie temperatures of the specimens of 10, 12, 16 and 35 at % B were determined to be 476, 524, 620 and 736 K, respectively. The T_c of amorphous alloys in the range between 20 and 33 at % B cannot be determined exactly, because crystallization occurs at a lower temperature than T_c. However, the Curie temperatures of x = 20 and 33 could be estimated to be 691 and 785 K, respectively, without large error, because $T_c \approx T_x$.

As can be seen in Fig. 11, T_c seems considerably higher than T_x in the specimens of x = 24 to 31. In such a case, T_c is usually determined from an extrapolation of the magnetization at low temperatures by using the Brillouin function or M^2–T curve. Properly speaking, these methods require a saturated state of magnetization in the specimen. It was hard to verify whether the magnetization of the specimens was saturated, because the applied magnetic field was relatively low ($\sim$ 0.1 T) in this experiment. Nevertheless, T_c was determined by extrapolating from the M^2–T curve on the assumption that the magnetization of the specimen was saturated, since the direction of the applied magnetic field was selected as parallel to that of the length of the ribbon.

For x = 10, T_c of the amorphous phase should be carefully determined, because excessive crystal phases are contained in the as-quenched specimen as mentioned before, the magnetization decreased around 470 K and increased again from 530 K as a result of the decomposition of the amorphous phase. The crystal phases should hardly influence the magnetization change around 470 K because the T_c values of the crystal phases are much higher than 470 K, i.e. 1043 for α-Fe and 897 K for o-Fe_3B. Therefore, the decrease of magnetization in the vicinity of 470 K is concluded to indicate the Curie temperature of the amorphous phase.

It can be pointed out in Fig. 12 that the T_c of x = 10 locates on the extrapolated line of Curie temperatures which decrease linearly with decreasing boron content in the range $12 \leq x \leq 20$. Furthermore, the first crystallization temperature T_{x1} for x = 10 also lies on the linear extrapolated line of T_{x1}. Therefore, the concentration of the amorphous phase

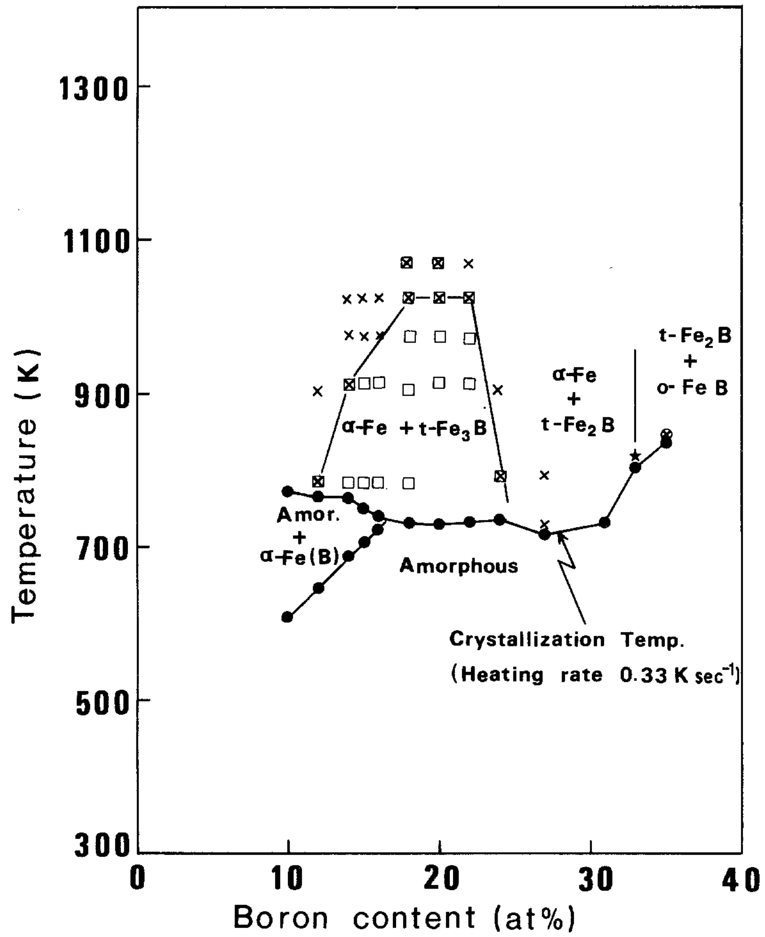

Figure 10 Crystallization phase diagram of liquid-quenched Fe–B amorphous alloys determined by these experiments. (x) α-Fe + t-Fe$_2$B, (□) α-Fe + t-Fe$_3$B, (⊠) α-Fe + t-Fe$_3$B + t-Fe$_2$B, (⊗) t-Fe$_2$B + o-FeB, (★) t-Fe$_2$B.

in the as-quenched specimen of $x = 10$ is concluded to be the same as its original value.

The concentration dependence of the Curie temperature is interpreted as follows. The decrease of T_c in the low-boron range closely relates to the structure of the amorphous alloy, that is, the structure of the alloy will approach to that of pure amorphous iron with decreasing boron content. It is inferred that the atomic arrangement of the amorphous iron will possibly have a similarity with the fcc structure rather than bcc from the point of view of the coordination number and the density. Therefore, the Curie temperature of the iron–boron alloy is suggested to be reduced by a decrease of ferromagnetic interaction because of the

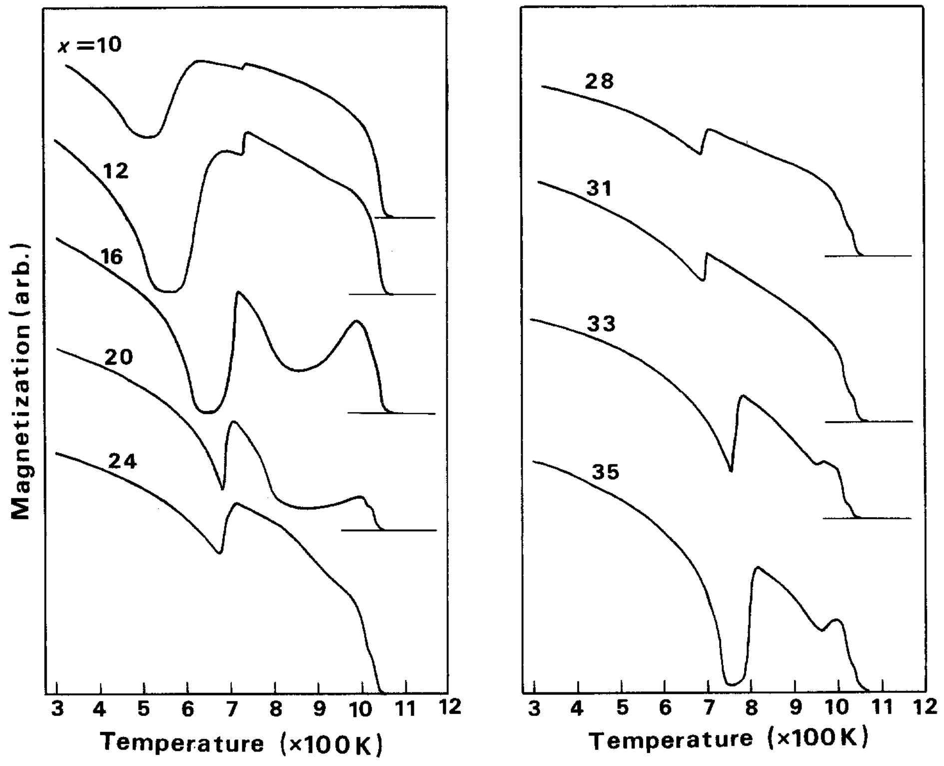

Figure 11 Magnetization against temperature curves for the as-quenched Fe$_{100-x}$B$_x$ (x = 10 to 35 at % B) alloys.

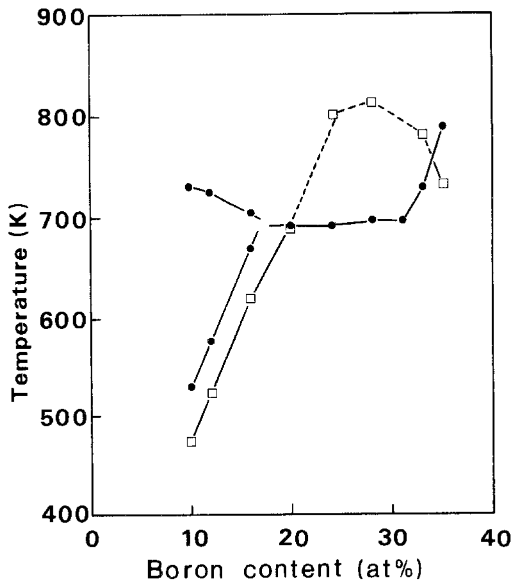

Figure 12 (□) Curie temperatures (T_c) and (●) crystallization temperatures (T_x) determined from the magnetization measurements (heating rate: 0.028 to 0.036 K sec^{-1}).

reduction of the iron–iron distance. Similarly, a lowering of T_c is observed in other amorphous alloys such as Fe–Zr [14] and Fe–Nd [15], and the spin glass behaviour of these alloys is noteworthy. On the other hand, the decrease of T_c in the high-boron range corresponds to a decrease of magnetic hyperfine field [9] and probably of the magnetic moment of iron, caused by an effect of metalloid boron atoms.

3.4.2. *Information on crystallization*

Crystallization temperatures were also determined from the magnetization measurements. Here, the crystallization temperature is defined as a middle point of magnetization change.

Two-step crystallization with broad (T_{x1}) and sharp (T_{x2}) changes in magnetization was observed in the magnetization against temperature curves of $x = 10$ to 16. For the specimens of $x = 10$ and 12, the magnetization change is a monotonically decreasing function in the temperature region above T_{x2}, which is due to the temperature dependence of the magnetization of α-Fe and Fe-B compounds. However, in the specimen of $x = 16$, the magnetization decreases in the vicinity of 800 K and increases again at ca. 870 K. The decrease in magnetization at ca. 800 K is considered to be due to the magnetic transition of t-Fe_3B from the results of other structural analyses, and the increase at ca. 870 K corresponds to the decomposition of t-Fe_3B to stable α-Fe and t-Fe_2B. The Curie temperatures of t-Fe_2B and α-Fe are higher than 1000 K. Such a change in magnetization is also observed in the specimen of $x = 20$.

The crystallization temperature in the boron range of $x = 20$ to 31 was determined to be ca. 700 K and nearly constant in accordance with the results of thermal analysis. In any composition for $x = 24$ to 31, the temperature dependence of magnetization above T_x is almost the same, where the phases consist of α-Fe and t-Fe_2B. The crystallization temperature shifted to the high temperature side in the specimens of $x \geqq 33$, and it was shown that T_x was higher than T_c at the concentration of $x = 35$.

An unexpected increase in magnetization was observed at ca. 970 K in the specimens of $x = 33$ and 35 as shown in Fig. 11. This abnormal behaviour seems to be due to the reduction of boron atoms from the specimen during the measurement of magnetization, because not much α-Fe phase was detected by Mössbauer effect in the specimen after the measurement.

It is shown that T_x determined from the magnetic measurement is lower than that from thermal analysis by ca. 40 K (compare Figs 10 and 12). However, the values were obtained almost equal when both measurements were carried out at the same heating rate. For example, in the specimens of $x = 24$ and 35, crystallization temperatures determined from the differential scanning calorimetry are 691 and 787 K, respectively, when specimens were heated at a rate of 0.028 K sec^{-1}. On the other hand, T_x values measured by a magnetic balance at a heating rate of 0.032 ± 0.004 K sec^{-1} were 693 and 789 K, respectively, which were in good agreement with T_x determined from DSC within the error range.

4. Conclusions

Alloys of $Fe_{100-x}B_x$ ($4 \leqq x \leqq 40$) were quenched from the melt by a single-roller method in a vacuum. The specimens were examined by DSC, X-ray diffraction, Mössbauer spectroscopy and magnetic balance.

1. The as-quenched state in this experiment was determined as follows:

$x = 4, 6$: α-Fe + o-Fe_3B

$x = 8$: α-Fe(B) + o-Fe_3B

$x = 10$: amorphous + α-Fe(B) + (o-Fe_3B?)

$x = 12$ to 35: amorphous

$x = 38, 40$: t-Fe_2B + o-FeB

2. The lattice parameter of the bcc solid solution with boron supersaturation in the 8 and 10 at % B alloys was 0.2861_0 nm (at 298 K), which was smaller by 0.2% than that of pure iron (0.2866_1 nm). Boron atoms were concluded to occupy substitutional sites in the bcc lattice.

3. Crystallization of $Fe_{100-x}B_x$ amorphous alloys progressed by the following reactions:

$x = 12$: amorphous → amorphous + α-Fe(B) → α-Fe + t-Fe_3B + t-Fe_2B → α-Fe + t-Fe_2B

$x = 14$ to 16: amorphous → amorphous + α-Fe(B) → α-Fe + t-Fe_3B → α-Fe + t-Fe_3B + t-Fe_2B → α-Fe + t-Fe_2B

$x = 18$ to 22: amorphous → α-Fe + t-Fe_3B → α-Fe + t-Fe_3B + t-Fe_2B → α-Fe + t-Fe_2B

$x = 24$: amorphous $\rightarrow$ α-Fe + t-Fe_3B + t-Fe_2B $\rightarrow$ α-Fe + t-Fe_2B

$x = 28$ to 31: amorphous $\rightarrow$ α-Fe + t-Fe_2B

$x = 33$: amorphous $\rightarrow$ t-Fe_2B

$x = 35$: amorphous $\rightarrow$ t-Fe_2B + o-FeB

4. The lattice parameter of the b c c phase, observed for the specimen of $x = 12$ at temperatures (673 K and 703 K) between the first and second crystallization temperatures, was 0.2860_0 nm (at 292 K), which is smaller than that of pure iron. The supersaturated boron atoms in the α-Fe(B) were transferred to the compounds at the time of the second crystallization reaction.

5. The crystallization temperature of $Fe_{100-x}B_x$ amorphous alloys ($10 \leqq x \leqq 35$) increased steeply at the concentration of $x = 33$. The value 835 K for $x = 35$ was 100 K higher than those for $18 \leqq x \leqq 31$.

6. The temperature at which the metastable phase (t-Fe_3B) changed to the stable phases (α-Fe + t-Fe_2B) depended sensitively on the boron content. The highest temperature of the phase transition was around 1000 K at $x = 20$.

7. The Curie temperature of the amorphous phase increased with increasing boron content up to $x = 28$, and then decreased. This behaviour is discussed in connection with the atomic and magnetic structure of the amorphous alloys.

Acknowledgements

We thank Dr K. Shiratori, Faculty of Science, Osaka University, for advice in the analysis of the magnetization curves and Mr T. Koyano, University of Tsukuba, for assistance in the measurement of magnetization.

References

1. U. HEROLD and U. KÖSTER, *Z. Metallkde.* **69** (1978) 326.
2. T. KEMENY, I. VINCZE, B. FOGARASSY and S. ARAJS, *Phys. Rev. B* **20** (1979) 476.
3. M. TAKAHASHI, M. KOSHIMURA and T. ABUZUKA, *Jpn. J. Appl. Phys.* **20** (1981) 1821.
4. K. NAGATA, T. HOSOMA and H. INO, in Proceedings of 4th International Conference on Rapidly Quenched Metals, Sendai, 1981, edited by T. Masumoto and K. Suzuki (Japan Institute of Metals, Sendai, 1982) p. 635.
5. H. INO, H. ICHINOSE and K. NAGATA, in Proceedings of 5th International Conference on Rapidly Quenched Metals, Würzburg, 1984, edited by S. Steeb and H. Warlimont (Elsevier, 1985) p. 263.
6. K. NAGATA and H. INO, *Nippon Kinzoku Gakkaishi* **49** (1985) 402 (in Japanese).
7. R. HASEGAWA and R. RAY, *J. Appl. Phys.* **49** (1978) 4174.
8. R. RAY and R. HASEGAWA, *Solid State Commun.* **27** (1978) 471.
9. T. NAKAJIMA, I. NAGAMI and H. INO, *J. Mater. Sci. Lett.* **5** (1986) 60.
10. R. RAY, R. HASEGAWA, C. P. CHOU and L. A. DAVIS, *Scripta Metall.* **11** (1977) 973.
11. W. HOVING, F. van der WOUDE, K. H. J. BUSCHOW and I. VINCZE, *J. Non-Cryst. Solids* **61/62** (1984) 421.
12. F. KANAMARU, S. MIYAZAKI, M. SHIMADA, K. ODA and Y. MIMURA, *J. Solid State Chem.* **49** (1983) 1.
13. U. KÖSTER and U. HEROLD, in "Topics in Applied Physics", Vol. 46, edited by H. J. Güntherodt and H. Beck (Springer, Berlin, 1981) pp. 225–259.
14. H. HIROYOSHI and K. FUKAMICHI, *J. Appl. Phys.* **53** (1982) 2226.
15. K. SHIRATORI, K. NAGAYAMA, H. INO, N. SAITO and Y. NAKAGAWA, in Proceedings of Intermag. Conference '87, Tokyo, 1987.

Received 6 April
and accepted 18 June 1987